



Chiang Mai J. Sci. 2019; 46(2) : 387-407
<http://epg.science.cmu.ac.th/ejournal/>
Contributed Paper

Synthesis and Characterization of Admicelled Natural Rubber with Poly(methyl methacrylate)-co-Poly((3-trimethoxysilyl) propyl methacrylate) and Evaluation of the Properties of its Vulcanizates

Suparat Nooma [a] and Rathanawan Magaraphan* [a,b,c,d]

[a] The Petroleum and Petrochemical College, Chulalongkorn University, Bangkok 10330, Thailand.

[b] Green Materials for Industrial Application Research Unit, Faculty of Science, Chulalongkorn University, Bangkok 10330, Thailand.

[c] Polymer Processing and Polymer Nanomaterials Research Unit, Petroleum and Petrochemical College, Chulalongkorn University, Bangkok 10330, Thailand.

[d] Center of Excellence on Petrochemical and Materials Technology, Chulalongkorn University, Bangkok 10330, Thailand.

*Author for correspondence; e-mail: rathanawan.k@chula.ac.th; krathana@gmail.com

Received: 9 May 2018

Revised: 22 August 2018

Accepted: 27 August 2018

ABSTRACT

Admicelled natural rubber (adNR) vulcanizates were prepared from NR modified by coating with poly(methyl methacrylate)-co-poly((3-trimethoxysilyl) propyl methacrylate), PMMA-co-PMPS shell. The core-shell structure of adNR was achieved after admicellar polymerization, using PMMA at 10 parts per hundred rubber (phr) and PMPS at 0-50 phr miscible in the mixture. During admicellar polymerization, hydrolysis and condensation of PMPS simultaneously with the free radical copolymerization of MPS and MMA give rise to the crosslink structure in the PMMA-co-PMPS shell, and these formations were assessed by FT-IR and H-NMR. The thermal stability of adNR was enhanced by the Si in PMMA-co-PMPS shells acting as an efficient diffusion barrier that hindered random scission of the polymer chains. The adNR vulcanizates were prepared by using conventional sulfur vulcanizing system. The mechanical properties, dynamic mechanical properties and swelling resistance improved with vulcanization and these were further enhanced by the PMMA-co-PMPS in the coating shell. The PMMA coating (adNR with PMMA 10 phr, P10), also with a low amount of PMPS (adNR with PMMA 10 phr and PMPS 12 phr, P10-S12), did not significantly affect the ozone resistance. However, ozone resistance then increased with further PMPS content (adNR with PMMA 10 phr and PMPS 12, 37 and 50 phr, respectively; P10-S25, P10-S37 and P10-S50). This high ozone resistance of adNR arises from the poor access of ozone to the double bonds in NR, protected by the encapsulating coating.

Keywords: natural rubber, vulcanization, coating, admicellar polymerization, silicon containing polymer

1. INTRODUCTION

Natural rubber (NR) is a bio-based polymer obtained from the rubber trees (*Hevea Brasiliensis*). NR has excellent characteristics such as high tensile strength, high elongation at break, low heat built up and outstanding resilience [1, 2]. However, NR is an unsaturated hydrocarbon consisting mainly of *cis*-1, 4-polyisoprene units with a double bond in each unit. Its undesirable material characteristics include high sensitivity to get attacks by atmospheric oxygen and ozone, due to the reactive double bonds in the main chain [3], and poor solvent resistance due to the nonpolar nature. These inherent drawbacks of NR limit its range of applications. In prior research, various physical and chemical modifications have been used to both improve the properties and widen the applications of NR. In physical modifications of NR to overcome these drawbacks, rubber manufacturers either adjust the compounding formulation, blend NR with other synthetic rubbery materials, or add inorganic fillers. The modifications usually associated with the mechanical properties of NR. However, these processes may not always improve the properties sufficiently.

In chemical modifications, graft copolymerization of poly(methylmethacrylate) (PMMA) in sufficient amounts could not only improve some characteristics of NR such as polarity and adhesion properties, but also introduce strong characteristics not usually associated with NR, like hardness, high modulus, good aging properties, ozone resistance, and swelling resistance, as evidenced by several reports [4, 5]. As an alternative to grafting, synthesizing polymer particles with core-shell structure, by forming core-shell structure with PMMA, become a novel method to improve properties of NR such as thermal and ozone resistance [6, 7]. However, after mastication and vulcanization

the coating film transformed into a smooth surface providing phase separation of NR and PMMA, so the core-shell structure was lost. This transformation occurred during mixing and crosslinking processes due to the weakness of interactions between coating layer and core substrate. To improve stability of coating polymer so as to maintain the core-shell structure, the incorporation of polymer forming siloxanes generated by silane monomers into the coating layer was tested in this work. 3-trimethoxysilyl propyl methacrylate (MPS) silane monomer proved to be of great practical and theoretical interest. The alkoxy groups of MPS silane monomer could be hydrolyzed and condensed, forming polymer networks acting as crosslink sites for copolymer material [8, 9]. In this sense, blending poly(3-trimethoxysilyl) propyl methacrylate) (PMPS) and PMMA to balance between their different properties seems a good strategy for the development of new materials, to serve as coating films on NR. Polymer network as the shell layer is formed and NR core is locked in the shell by crosslinking PMPS and glassy PMMA, which stabilizes the structure during mixing and vulcanization [10].

To the best of our knowledge, there is no prior report regarding the synthesis PMMA-co-PMPS on NR by using admicellar polymerization. Admicellar polymerization, which is an innovative technique, can be applied to adjust the surface properties of NR in latex form by nanoscale coating with a suitable polymer. The obtained admicelled NR (adNR) shows strong polymeric shell adherence to NR substrate without chemical bonds. The application of admicellar polymerization was also reported by several researchers [11-13]. For example, NR coated by acrylic acid (AA) copolymerization with modified silica from 3-trimethoxysilylpropyl

methacrylate (MPS) showed better ionic conductivity [14], while polystyrene (PS) improved processibility [15], and polypyrrole (PPy) improved electrical conductivity [16].

Therefore, in this work aimed to modify NR with PMMA-co-PMPS copolymer by using admicellar polymerization method, to develop novel materials with adjustable thermal and oxidative properties. The effects of monomer concentration on chemical, thermal, and morphological properties were investigated. Then, the adNR was further vulcanized using sulfur vulcanizing system. The reinforcement effects of PMMA-co-PMPS were investigated by assessing dynamic mechanical properties, mechanical properties, and aging resistance. In addition, swelling ratios were determined to assess solvent resistance, and the density of ozone induced cracks on adNR surfaces is also reported.

2. MATERIALS AND METHODS

2.1 Materials

NR latex was high ammonia with 60 wt% dry rubber content from the Rubber Research Institute, Thailand. MMA monomer with 99% purity and hexadecyltrimethylammonium bromide (CTAB) with 97% purity were purchased from Merck, Germany. MPS silane monomer with 98% purity and potassium peroxodisulfate (KPS) initiator were received from Fluka, Germany. All of the above were used as received as the

primary materials. The commercial additives sulfur (S), zinc oxide (ZnO) and stearic acid were purchased from Bayer, Germany; and N-tert-butyl-2-benzothiazolesulfenamide (TBBS) was purchased from Flexsys, United States. All additives were used as received without further purification.

2.2 Methods

2.2.1 Admicellar polymerization of NR with PMMA-co-PMPS

The admicellar polymerization of NR (5 wt%) with MMA and MPS silane monomers (the compositions are listed in Table 1) was carried out at pH 8 (1 M HCl was used to adjust pH) in an aqueous solution of CTAB at the equilibrium concentration of 800 mM to avoid emulsion polymerization [7]. Then MMA monomer was added into the mixture and stirred at room temperature (30 °C) for 24 h. After that, MPS silane monomer was added into the mixture and stirred at room temperature for 24 h. Next, KPS initiator (0.01 wt% relative to monomers) was added into the mixture to initiate polymerization. The admicellar polymerization was carried out at 90 °C for 9 h under nitrogen purge, producing adNR [12]. The obtained adNR was separated by centrifugation, washed with distilled water to remove excess CTAB, and dried in a vacuum oven at 70 °C, before further use in the characterizations.

Table 1. The experimental compositions tested.

Samples	Parts per hundred rubber (phr)			Composition of adNR [%wt]		
	NR	MMA	MPS	NR	PMMA	MPS
P10	100	10	-	90.91	9.09	-
P10-S12	100	10	12	81.96	8.20	9.84
P10-S25	100	10	25	74.07	7.41	18.52
P10-S37	100	10	37	68.03	6.80	25.17
P10-S50	100	10	50	62.50	6.25	31.25

2.2.2 Preparation of adNR compounds

The compounding process was initiated by masticating rubber on a laboratory two-roll mill (Labtech LRM 110 model) for 5 min. The initial roll temperature was set at 40 °C by using the circulation of water. The compounding time on the mill was 20 min to ensure uniform distribution of the ingredients; this as well as the sequence of adding ingredients were kept constant across all cases. The ingredients were added in the sequence: rubber, zinc oxide, stearic acid, TBBS, and sulfur. The formulations used are shown in Table 2. The compounds were named as P10-Sxx where P10 is the adNR with PMMA 10 phr, S refers to MPS silane monomer and xx is the variable content of MPS silane monomer added in the NR latex.

Table 2. Formulation of compounds with curing ingredients.

Materials	Amount used (phr*)	
	Control	Samples
AdNR	-	100
NR	100	-
Zinc oxide	5	5
Stearic acid	1	1
TBBS	1	1
Sulfur	3	3

* phr = parts per hundred rubber

2.2.3 Vulcanization process

The compounded adNR was cured in a hydraulic compression molding machine (Labtech LP20 model) at 150 °C at an applied pressure of 10.00 MPa, in each case for the respective optimum cure time ($t = t_{c90}$) obtained from rheographs. The cure temperature was fixed while the t_{c90} was varied by case. After curing, the sheet of adNR vulcanizate was immediately cooled with water to stop further curing and then

taken out of the mold. The samples were stored at room temperature for 24 h before testing.

2.3 Characterization of adNR

2.3.1 Composition of adNR

Quantitative extraction of adNR was done by using a Soxhlet apparatus. Two grams of adNR were put into a cellulose extraction thimble, and inserted in the Soxhlet extractor containing 100 ml of extracting solvent. The extraction steps used petroleum ether, acetone and methanol to remove free NR, free PMMA and free PMPS, respectively. To remove free NR, the sample was extracted with petroleum ether at 70 °C for 24 h, and then dried at 60 °C in vacuum oven for 24 h. Then, free PMMA was removed by extraction with acetone at 230 °C for 6 h, and the residue was dried at 60 °C in a vacuum oven for 24 h. After that, free PMPS was also removed by extraction with methanol at 230 °C for 6 h, and the residue was dried at 60 °C in vacuum oven for 24 h. The sample was weighed after drying in each extraction step, and the composition in terms of free NR, free PMMA, free PMPS and adNR is reported in Table 3.

2.3.2 X-ray photoelectron spectroscopy

X-ray Photoelectron Spectroscopy (XPS, Kratos Axis Ultra DLD model, with monochromated aluminum (Al) K α source) was used to obtain both qualitative and quantitative information on the elemental composition of adNR. Samples were examined as the method described by Park *et al.* [17]. The survey scans for wide scan analysis were taken with 160 eV pass energy for each sample. The high-resolution narrow scans were recorded with 40 eV pass energy for each element detected in each sample. The emission angle from the X-ray detector with respect to the sample surface was 90°.

This corresponds to a maximum sampling depth of about 10 nm. The analyzed area and base pressure were $700 \times 300 \text{ mm}^2$ and $3 \times 10^{-9} \text{ Torr}$, respectively. Peak intensities were determined by integrating each peak area. Sensitivity factors were used (0.25 for C_{1s} , 0.66 for O_{1s} , and 0.42 for Si_{2p} , respectively) to normalize the peak areas. Fitting of the C_{1s} peak at 285.0 eV was carried out with a Gaussian curve-fitting program. The composition by atomic species was calculated according to the formula below [18], where C_i expresses the relative mole content; A_i is peak area; and S_i is sensitivity coefficient (0.25, 0.66 and 0.42 were adopted for C, O and Si, respectively).

$$C_i = \frac{A_i / S_i}{\sum A_i / S_i} \quad (1)$$

2.3.3 FT-IR spectroscopy

Chemical structure was investigated by Fourier Transform Infrared Spectrometry (FT-IR), with a Nicolet Nexus 670 spectrometer. The adNR was mixed with KBr and ground in a mortar to a fine mixture, which was transferred into a die-set and pressed at 7 bars for 2 min to make a pellet. Each sample was measured with 16 scans in $4000\text{--}650 \text{ cm}^{-1}$ range with 4 cm^{-1} resolution.

2.3.4 H-NMR spectroscopy

In order to assess the reactions of MPS silane monomer, and the hydrolysis and condensation, chemical structure of the adNR was also characterized by using a Nuclear Magnetic Resonance (NMR) Spectrometer, model VNMRS 400 Agilent Technologies, with the H-NMR technique. The samples were dissolved in deuterated chloroform ($CDCl_3$) at room temperature and kept in tightly capped bottles. The samples were put in 5 mm glass NMR tubes to 4.5 cm height. The NMR spectra were recorded at 400 MHz.

2.3.5 Thermogravimetry measurement

Thermal stability of NR, PMMA, PMPS and adNR was assessed from Thermogravimetric analysis (TGA) with a High Resolution TG-DTA Pyris Diamond, Perkin Elmer. During measurement each specimen was placed in a platinum pan and heated from $30 \text{ }^\circ\text{C}$ to $800 \text{ }^\circ\text{C}$, under 100 ml/min nitrogen purge, at a heating rate of $10 \text{ }^\circ\text{C/min}$.

2.3.6 Morphological study

The core-shell structure of adNR was imaged with a Transmission Electron Microscope (TEM), model JEM-2100 at an accelerating voltage of 100 kV with a magnification of 10,000x. The samples were prepared by dropping diluted emulsion on a copper (Cu) grid and drying at ambient temperature. In addition, a Field Emission Scanning Electron Microscope (FE-SEM), model Hitachi S-4800, was also used to observe the morphology of adNR at accelerating voltage of 5.0 kV and magnification of 5000x. Cryo-fractured surfaces were prepared by immersion in liquid nitrogen and were sputter coated with a thin layer of platinum under vacuum before observation.

2.4 Characterization of Cured adNR

2.4.1 Cure characteristics

Cure characteristics of NR and adNR compounds were measured by using a Moving Die Rheometer (MDR), rheoTECH MD+, according to ASTM D5289 at $150 \text{ }^\circ\text{C}$ under a constant frequency of 1.66 Hz and an oscillating rotation of 0.5° . The scorch time (t_{s1}), cure time (t_{c90}), cure rate index (CRI) and torque difference ($M_H - M_L$; where M_H is maximum torque and M_L is minimum torque) were determined for each case from the vulcanization curve. The results of the cure characteristics are listed in Table 6.

2.4.2 Swelling test

Swelling behavior was determined gravimetrically according to ASTM D471-06 in toluene for 5 days. The mole uptake of solvent, swelling ratio, soluble fraction were reported and crosslink density was estimated by using Flory-Rehner equation [19]. The volume fraction (V_r) of rubber in the swollen samples was calculated from:

$$V_r = \frac{1}{1 + \frac{\rho_r}{\rho_s} \left(\frac{W_s - W_d}{W_d} \right)} \quad (2)$$

where ρ_r and ρ_s are the densities of rubber and solvent, respectively. The Flory solvent-polymer interaction parameter (χ) was determined from:

$$\chi = 0.44 + 0.18V_r \quad (3)$$

The molecular weight between crosslinks (M_c) was determined as follows:

$$\frac{1}{M_c} = - \frac{1}{2\rho_r V_o} \left[\frac{(h(1-V_r) + V_r + \chi V_r^2)}{(V_r^{\frac{1}{3}} - \frac{1}{2} V_r)} \right] \quad (4)$$

where V_o is the molar volume of solvent absorbed (toluene $V_o = 106.3 \text{ cm}^3/\text{mole}$). Then, the crosslink density (ν) can be determined from the following relation:

$$\nu = \frac{1}{2M_c} \quad (5)$$

2.4.3 Ozone resistance testing

Ozone resistance of NR and adNR vulcanizates was measured according to ISO 1431-1. The specimens with 2 mm thickness were prepared by compression molding and cutting to 20 mm (width) \times 80 mm (length). They were stretched and held at 20% elongation while kept in a dark room for 48 h, before exposure to 0.50 ppm (parts per million) of ozone (O_3) atmosphere at 40 °C for 24 h. Five replicates are tested.

After exposure to O_3 , the cracks on surface of each sample were photographed by an Optecstereo microscope model SZ760B2L with a magnification of 10 \times .

2.4.4 Mechanical properties and aging

Tensile strength, modulus and elongation at break of NR and adNR vulcanizates were done with an Instron model 33R4206 universal testing machine, with a cross-head speed of 500 mm/min and 1 kN load cell at room temperature. Specimens were punched out of the molded sheet with a dumbbell-shaped die in accordance with ASTM D412 type C with a gauge length of 33 mm. Averages of at least five replicates are reported.

Thermal aging of NR and adNR vulcanizates was done at 70 °C for 96 h, according to ASTM D573. The accelerated aging effects were measured 24 h after aging. Tensile strength, modulus and elongation at break from at least five replicates are reported.

2.4.5 Dynamic mechanical properties

Thermal-mechanical properties of NR and adNR vulcanizates were evaluated using a Dynamic Mechanical Analyzer (DMA), Gabo Explex or 100N model, at a frequency of 10 Hz and a heating rate of 2 °C/min. The specimen was prepared by compression molding and cutting to the size of 40 mm (length) \times 10 mm (width) \times 2 mm (thickness). Storage modulus (E'), loss modulus (E'') and loss tangent ($\tan \delta$) were determined as functions of temperature. The experiment was carried out from -100 °C to 150 °C in tension mode. The dynamic strain amplitude was $\pm 10 \mu\text{m}$ and the applied forces to maintain this amplitude were automatically controlled.

3. RESULTS AND DISCUSSION

3.1 Properties of adNR

3.1.1 Composition analysis of adNR

The composition in weight percentages of adNR obtained from Soxhlet extraction, compared to the monomer contents in Table 1, is given in Table 3. It can be clearly seen that higher silane content increases the yield of adNR. All adNR samples had comparatively large admicelled part, ensuring

that the admicellar polymerization on NR of PMMA-co-PMPS copolymer was successful. As due to the low solubilities of MMA and MPS silane monomers in water, the monomer adsolubilized into the surfactant bilayer template, increasing the conversion and deposition of monomers on NR cores, similar observation was reported by Pongpilaipruet *et al.* [7].

Table 3. Composition of adNR determined by solvent extraction.

Samples	Free polymer			AdNR (%wt)
	NR (%wt)	PMMA (%wt)	PMPS (%wt)	
P10	89.32	2.05	-	8.63
P10-S12	67.56	1.90	11.81	18.73
P10-S25	53.77	2.17	13.00	31.06
P10-S37	34.10	2.04	13.07	50.79
P10-S50	34.31	2.47	12.75	50.47

Table 4 shows the XPS survey results for NR and adNR, in terms of electrons of oxygen (O_{1s}), carbon (C_{1s}), and silicon (Si_{2p}). These elements occurred in the regions around 533, 285 and 103 eV, respectively. The C_{1s} is considered to mainly arise from

NR, while O_{1s} arise from both PMMA and PMPS, and Si_{2p} arise from PMPS. The peak areas in the survey spectra were normalized with sensitivity factors to obtain quantitative information on the elemental composition of adNR, shown in Table 4.

Table 4. Composition of adNR from XPS analysis.

Samples	Relative mole composition (%)			O/C ratio (%)	Si/C ratio (%)
	C	O	Si		
NR	100	-	-	-	-
P10	94.73	5.27	-	5.56	-
P10-S12	84.87	11.65	3.48	13.73	4.10
P10-S25	83.40	11.12	5.48	13.33	6.57
P10-S37	74.97	18.12	6.91	24.17	9.22
P10-S50	82.30	12.29	5.41	14.93	6.57

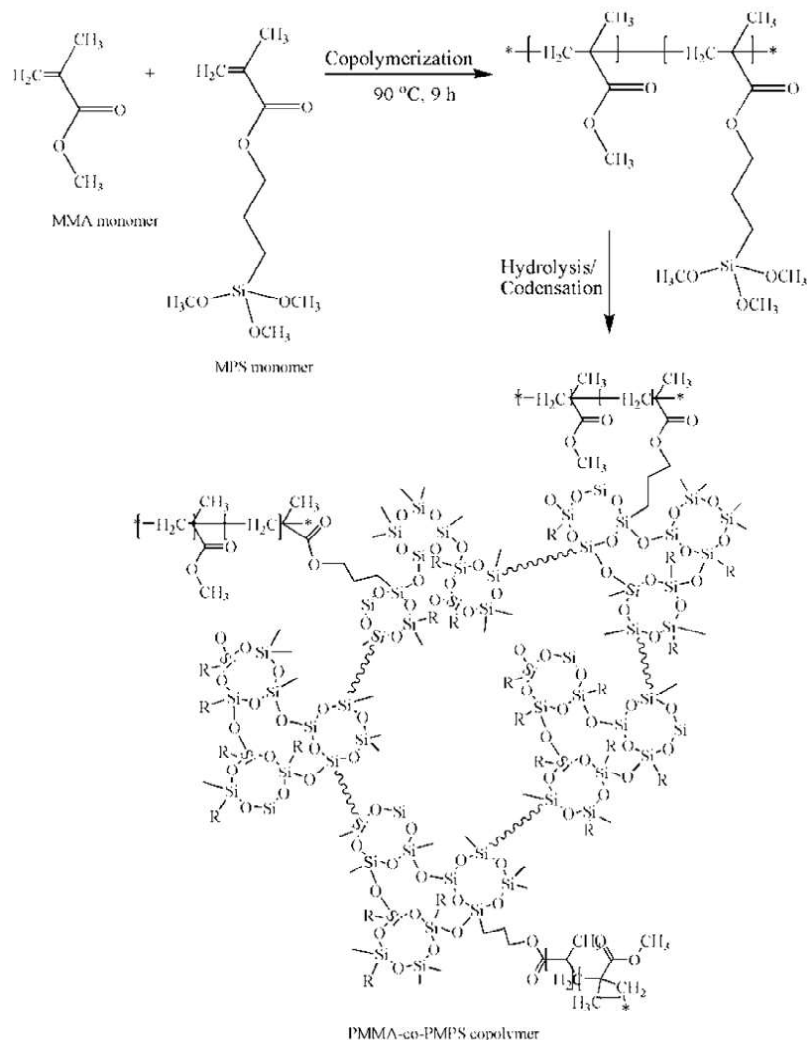
For NR, the carbon electrons gave 100% of the elemental composition. When NR was admicelled with PMMA-co-PMPS, the content of C_{1s} electrons decreased, which subsequently increased the relative contents of O_{1s} and Si_{2p} electrons. An increase

in the O/C and Si/C ratios indicates that the PMMA-co-PMPS was attached to the NR surfaces by admicellar polymerization. Similar observations were reported for admicelled polyisoprene-silica [20], admicelled polystyrene-cotton [12], admicelled

polystyrene-NR [15] and admicelled polyacrylate-NR [7]. However, increasing MPS silane monomer to 50 phr enhanced self-condensation reactions of methoxy groups of monomeric alkoxy silane. Thus, the conversion of PMPS on NR decreased as reported by the lower value of Si/C ratio of P10-S50.

During the admicellar polymerization, the-Si-(OCH₃) of PMPS could hydrolyze and condense to form siloxane linkages (-Si-O-Si-) depositing on the NR particles, as mentioned by Zaioncz *et al.* [21] and

Cai *et al.* [22]. The MPS silane and MMA monomers could be copolymerized via C=C bonds through free radical copolymerization while the methoxy groups of MPS could be hydrolyzed and condensed, forming polymer networks acting as crosslink sites, siloxane linkages, depositing on the NR particles. The hydrolysis and condensation of PMPS simultaneously with the free radical copolymerization of MPS and MMA gives rise to a crosslinked structure, as illustrated in Scheme 1.



Scheme 1. Proposed structure of the PMMA-co-PMPS copolymer.

3.1.2 FT-IR spectra of adNR

To ensure the formation of siloxane linkages (-Si-O-Si-), the structural features of adNR with PMMA-co-PMPS copolymer were investigated by FT-IR, as shown in Figure 1. In the case of PMMA, the wave number 1731 cm^{-1} represents the stretching vibrations of -C=O , while 1149 cm^{-1} corresponds to the stretching vibrations of -C-O . In the spectrum of PMPS, the symmetrical stretching vibrations of -Si-O-Si- and the absorption peak of -C=O appear at 1080 cm^{-1} and 1720 cm^{-1} , respectively.

The characteristic peaks of NR appearing at 832 cm^{-1} is attributed to the *cis*-1,4-polyisoprene configuration $\text{-C(CH}_3\text{)=CH-}$. The characteristic peaks of NR, PMMA and PMPS appeared in case of adNR. The absorption peaks at 832, 1731 and 1080 cm^{-1} correspond to $\text{-C(CH}_3\text{)=CH-}$, -C=O and -Si-O-Si- , respectively [23]. These absorption spectra corroborate successful admicellar polymerization of PMMA-co-PMPS on NR with the formation of siloxanes.

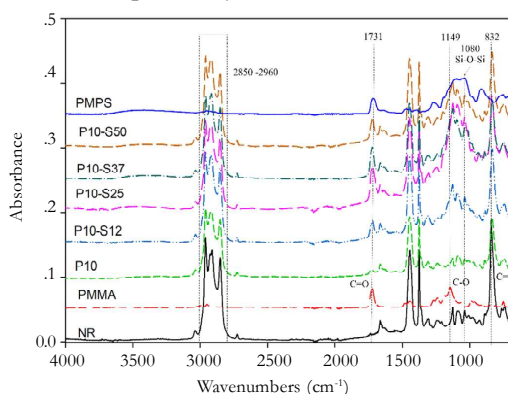


Figure 1. FT-IR spectra of NR, PMMA, PMPS and adNR.

3.1.3 H-NMR of adNR

As illustrated in Scheme 1, the hydrolysis and condensation of MPS simultaneously with the free radical copolymerization of MPS and MMA gives rise to a crosslinked structure. Thus, the structural features of the

PMMA-co-PMPS copolymer prepared in this study were investigated by H-NMR spectroscopy. Figure 2 presents the H-NMR spectra of adNR containing PMMA-co-PMPS.

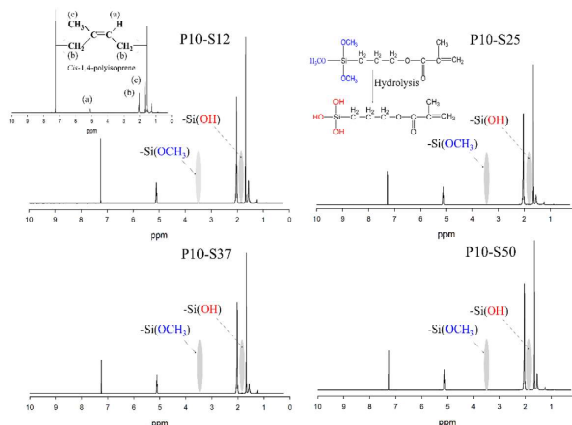


Figure 2. H-NMR spectra of NR and adNR.

The H-NMR spectrum of NR exhibits three resonance peaks at around 5.15 ppm, 2.10 ppm and 1.70 ppm, associated with unsaturated methyne protons, methylene protons and methyl protons, respectively. It is important to point out that the H-NMR spectra of adNR are consistent with high condensation degree of PMPS, which should react during the polymerization. The copolymerization of MMA and MPS resulted in the disappearance of the protons of $-\text{Si}(\text{OCH}_3)_3$ and $-\text{Si}(\text{OH})$ at 3.48 and 1.83 ppm, respectively; by complete condensation of the MPS silane monomers. It is well-known that alkaline pH with high temperature, as in this study, promotes hydrolysis and condensation of alkoxy silane. As a consequence, during the synthesis of PMMA-co-PMPS copolymer, the hydrolysis of the methoxy groups of the MPS occurs first, followed by the condensation of hydroxyl groups to form siloxane linkages in PMMA-co-PMPS copolymer. Therefore, the PMMA chains linked to the inorganic siloxane particles forming an organic-inorganic copolymer covering of NR, similarly as reported by Zaioncz *et al.* [21].

3.1.4 Morphological study of adNR

TEM micrographs of NR and adNR particles are shown in Figure 3. Round shaped NR particles with a diameter of about 1.0 μm are seen in Figure 3a. TEM micrographs of adNR exhibit clearly differentiated dark NR particles surrounded by a thin layer of grey PMMA-co-PMPS, in Figure 3b-e. The polymer shell deposits fully covered the NR particle with a rough surface and non-uniform thickness of around 100 - 300 nm. With increasing PMPS, size of adNR increased due to increasing shell thickness. This demonstrates the core-shell structure on NR particles coated after admicellar polymerization [7, 14].

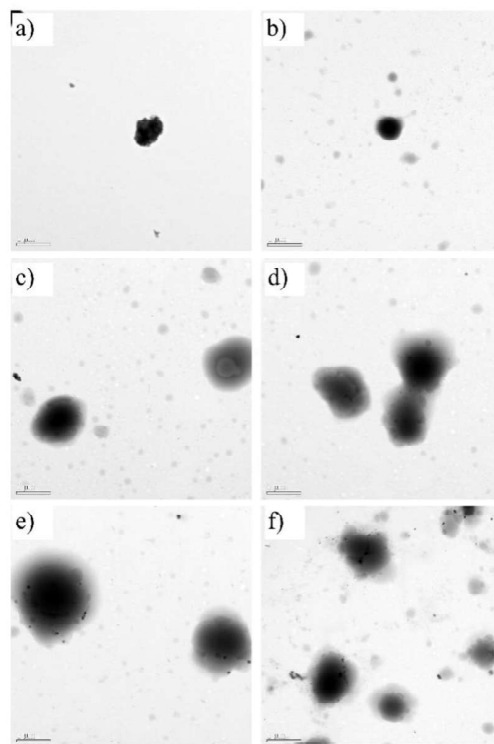


Figure 3. TEM micrographs of NR and adNR; a) NR, b) P10, c) P10-S12, d) P10-S25, e) P10-S37 and f) P10-S50.

FE-SEM micrographs reveal the morphology of NR and adNR in drying state. Smooth surfaces with only carbon atoms are observed for NR due to its hydrocarbon nature, as seen in Figure 4a. The NR particles were fused together and formed homogenous flat surfaces during drying because of the low T_g ($\sim -72^\circ\text{C}$) of NR [7]. After modification, the adNR with PMMA shows rather rough surfaces with well distributed C and O atoms in the FE-SEM-EDX mapping of Figure 4b. In the case of the adNR with PMMA-co-PMPS, rough surfaces are still obviously observed in all tested samples, with an average particle size of about 0.45 - 7.5 μm . More agglomerated particles are observed with higher content of PMPS, as seen in Figure 4c-f. This result shows the effects of T_g . Since PMMA and PMPS

have rather high T_g , their presence as a rigid shell covering NR particles prevents NR fusion, and the particle aggregates were still present after drying [7]. In addition, as silane monomer could react with C=C of PMMA and methoxy terminated groups could also play a role of crosslinking agent forming siloxane domains in the shell layer, resulting in a more stable of core-shell structure polymer [24, 25]. This morphology was

possibly improved stability and maintained core-shell structure during processing. The siloxane domains were confirmed by the detection of Si atoms, which were clearly observed in the FE-SEM-EDX results as particles on the fracture surfaces. The Si atoms in FE-SEM-EDX mapping show good and uniform distribution in the adNR samples, indicating improved dispersion and compatibility of Si in NR matrix.

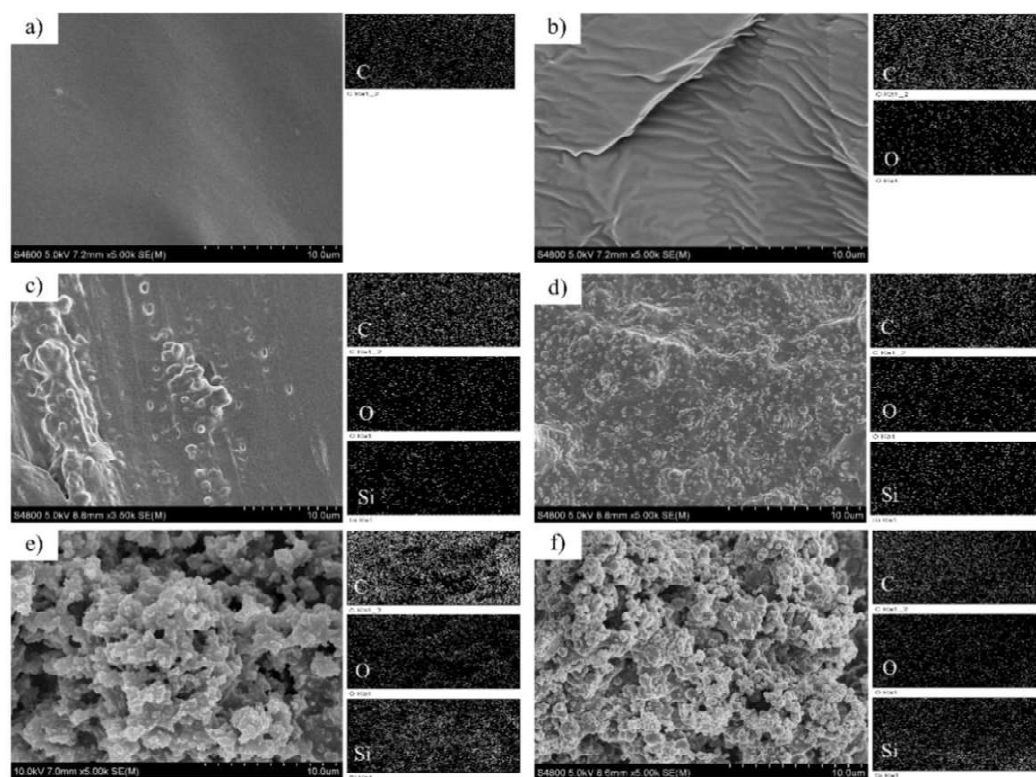


Figure 4. SEM images with EDX mapping of NR and adNR; a) NR, b) P10, c) P10-S12, d) P10-S25, e) P10-S37 and f) P10-S50.

3.1.5 Thermal properties of adNR with PMMA-co-PMPS

Thermal properties of NR, PMMA and PMPS are shown in Figure 5. NR and PMMA decomposed in one step at 338.39 and 341.83 °C, respectively. Although the decomposition temperature of PMMA in multi-step was reported by several studies, there were some studies reported that

PMMA showed a one-step decomposition pattern in range of 312-433 °C [7]. In case of PMPS, the decomposition temperature shifted to significantly higher temperature (396.2 °C) indicated better thermal stability than those of NR and PMMA and the greater amount of char residue from PMPS is due to the present of inorganic silicon element [26].

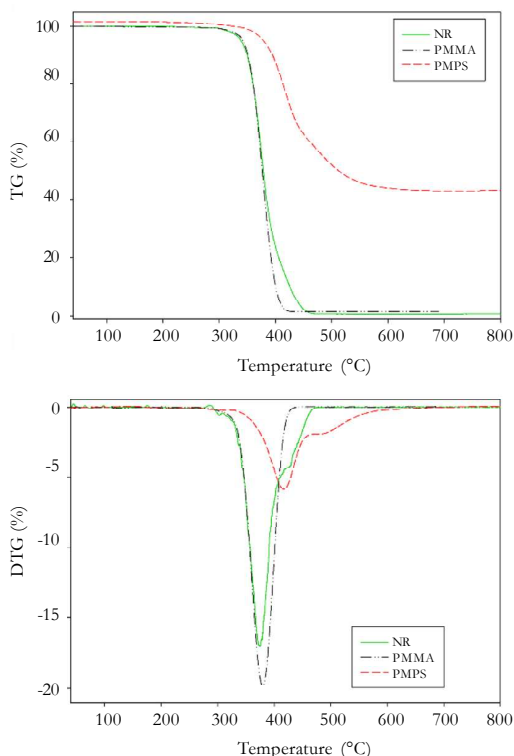


Figure 5. TG and DTG of NR, PMMA and PMPS.

Figure 6 shows the TG and DTG curves of the adNR. The decomposition temperature of adNR (342.73-347.22 °C) was significant higher than that of NR (338.39 °C) and was improved by PMPS loading, as summarized in Table 5. Especially at high weight loss levels (see T_{30} , T_{50} and T_{70}), the TG curves were obviously increased and the decomposition temperatures of adNR were higher than that of NR about 17-27 °C because the decomposition was retarded by silicon containing polymer shell which effectively reduced the diffusion of heat to the core NR and provided higher thermal stability.

The improvement is attributed to the good thermal stability of siloxane domains in the shells of adNR. The TG and DTG for adNR showed one distinct peak with a small shoulder of DTG at high temperature, similar to the decomposition of admicelled PS-NR [15], admicelled PMA-NR and PMMA-NR [7]. This result indicated that good interaction and compatibility between two phases was provided by admicellar polymerization. The maximum decomposition temperature ($T_{d(max)}$) around 374-377 °C reflects polymeric decomposition of NR, and the shoulder at higher temperature indicates decomposition of siloxane domains at about 411 °C which closes to the $T_{d(max)}$ of PMPS at 416 °C. Importantly, based on the mass of char residue, the higher amount of char from adNR than the expected value suggests that the thermal stability of adNR was improved by adding PMPS due to the formation of siloxanes which lead to stiffening of polymer chain in the shell part [24, 25]. Moreover, the flame retardant of adNR was enhanced by the presence of Si element, which is a trivalent metalloid with low reactivity and high thermal stability. Therefore, the thermal stability of adNR was enhanced by the Si in the shells and by the crosslinks of siloxane linkages. Similar observation is reported by Cavalho *et al.* [26], with PMMA/polysiloxane hybrid material. The thermal stability improved because PMMA/polysiloxane acted as an efficient diffusion barrier to hinder random scissions of the polymer chains.

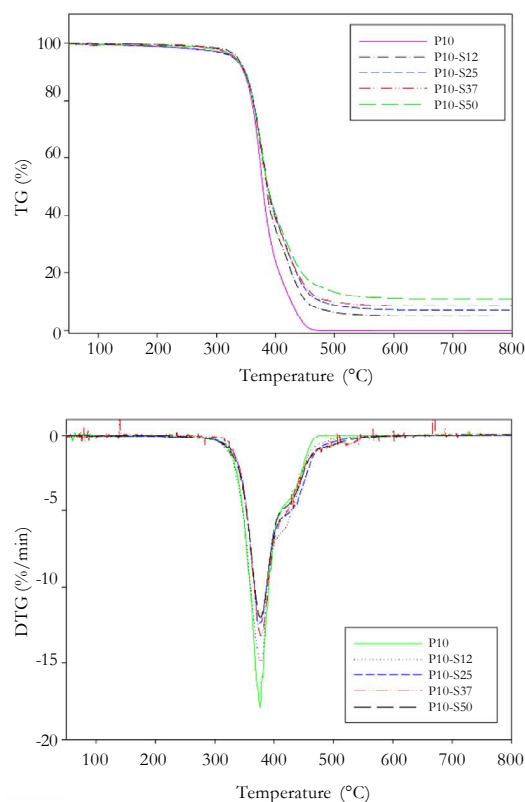


Figure 6. TG and DTG of adNR.

Table 5. Thermal properties of NR, PMMA, PMPS and adNR.

Samples	T_{onset} (°C)	$T_{\text{d(max)}}$ (°C)	T_{30} (°C)	T_{50} (°C)	T_{70} (°C)	Weight Loss (%)	Measured Residue (%)	Expected Residue (%)
NR	338.39	347.15	367.17	378.32	392.42	99.42	0.58	-
PMMA	341.83	379.70	366.27	376.57	386.10	98.64	1.36	-
PMPS	396.20	416.89	430.38	511.53	N/A	56.81	43.19	-
P10	338.67	376.56	367.34	378.11	392.83	99.92	0.08	-
P10-S12	342.73	377.30	371.21	385.23	409.13	95.16	4.84	2.38
P10-S25	343.99	377.46	371.83	387.09	413.14	93.19	6.81	4.48
P10-S37	347.22	377.30	372.00	387.79	415.60	91.47	8.53	6.09
P10-S50	349.10	377.30	372.49	388.36	419.92	89.11	10.89	7.56

3.2 Properties of Cured adNR

3.2.1 Cure characteristics of adNR compounds

The t_{c90} and t_{s1} of NR and adNR vulcanizates are presented in Table 6. The t_{s1} indicates the period which a rubber compound can be processed at a given

temperature before curing while the time required for the rubber compound to reach 90% of the state of cure is t_{c90} which can be varied depending on the type of rubber compound and the thickness of the product. In this experiment, the t_{s1} and t_{c90} of adNR were shorter than that of NR. However,

the t_{s1} and t_{c90} were almost unchanged in the case of adNR. This is due to the polar character of adNR surface, the $-\text{Si}(\text{OCH}_3)_3$ of PMPS could hydrolyze and condense to form siloxane linkages ($-\text{Si}-\text{O}-\text{Si}-$) depositing on the NR particles during the admicellar polymerization, that adsorbs the polar curatives and results in cure acceleration as well as vulcanization efficiency (see higher CRI of adNR). Similar reduction in scorch time and cure time with silane content was also reported by Nelson *et al.* [33] and Yan *et al.* [34].

The torque difference is a measure of dynamic shear modulus, which is related

indirectly to the crosslink density of the vulcanizates. It is observed in Table 6 that the torque difference increased with adding PMMA and PMMA-co-PMPS. The increase in torque difference was attributed to the formation siloxane linkages which indicates the extent of crosslinking of PMPS. The increased crosslink density of adNR vulcanizates is then reflected in the increasing of torque difference. The siloxane linkages are considered as the additional chemical crosslinks, and, together with the sulphide crosslinks, contribute to the total crosslink density in adNR vulcanizates.

Table 6. Cure characteristics of adNR compounds at 150 °C.

Samples	t_{s1} (min)	t_{c90} (min)	CRI	$M_H - M_L$ (N.m)
NR	3.01	8.19	18.81	5.30
P10	1.07	6.07	20.03	6.70
P10-S12	1.04	5.54	20.71	6.92
P10-S25	0.58	6.09	19.36	7.31
P10-S37	1.01	6.15	19.10	9.06
P10-S50	1.02	5.48	21.01	9.71

3.2.2 Morphological study of adNR vulcanizates

FE-SEM micrographs of NR and adNR vulcanizates are shown in Figure 7. During vulcanization, NR was fused and linked to a homogeneous matrix. In adNR vulcanizates, the core-shell structure was transformed upon mastication and vulcanization indicating that the NR core and PMMA-co-PMPS shell were physically bonded. However, the PMMA-co-PMPS shell has siloxane links covering the NR

particles, so rigid aggregate particles in NR matrix remain after the mastication and vulcanization, with approximate size range 400-800 nm. On increasing the concentration of PMPS in PMMA-co-PMPS shell, the domains of aggregates increased with uniform distribution and no void at the interphase was observed. This suggests that the admicellar polymerization method provides good adhesion even between materials with different polarities.

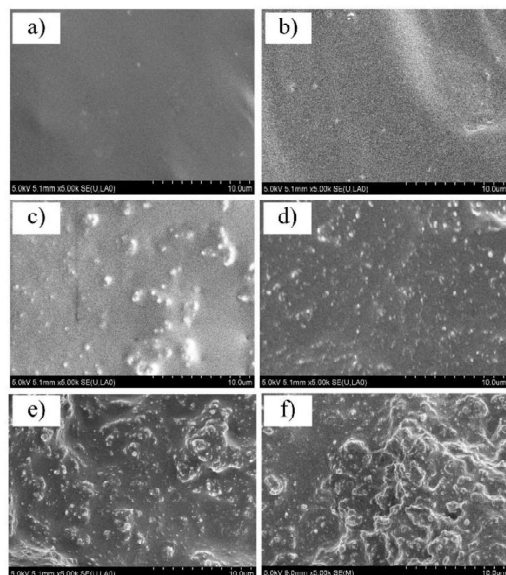


Figure 7. SEM images of NR and adNR vulcanizates; a) NR, b) P10, c) P10-S12, d) P10-S25, e) P10-S37 and f) P10-S50.

3.2.3 Ozone resistance of adNR vulcanizates

Ozone resistance was investigated by exposing NR and adNR vulcanizates to 0.50 ppm ozone concentration for 24 h. The ozone cracks at the surfaces of the specimens were photographed, as shown in Figure 8. Visible cracks were found for the case of NR, Figure 8a. Without coating NR was highly susceptible to ozone attack, and large and deep ozone cracks are found on the specimen surfaces [4, 27]. Coating with PMMA, Figure 8b, also with a low amount of PMPS, Figure 8c, did not significantly affect the ozone resistance. Although in the current study some cracks were found also in adNR, these were less severe than without coating: the cracks were smaller and discontinuous, instead of deep, wide and continuous. The ozone resistance of the vulcanizates consistently improved with PMPS content in the adNR, as illustrated in Figure 8d-f. The cracks in adNR are small and discontinuous suggesting improved ozone

resistance. This arises from the poor access of ozone to the double bonds in NR phase, which is protected by the polymer shell. Here the coating was formed by admicellar polymerization, with PMMA-co-PMPS.

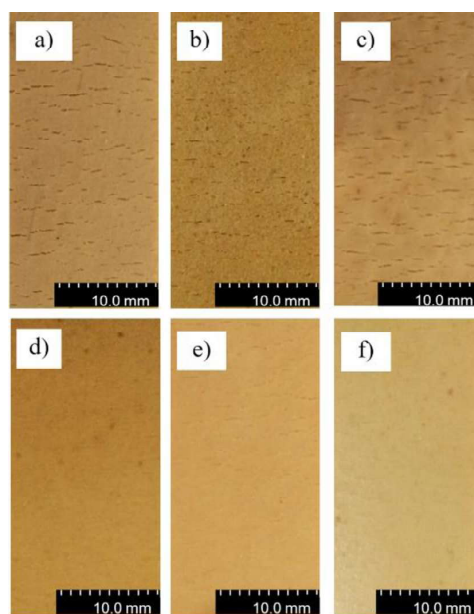


Figure 8. Optical photographs of ozone exposed surfaces of NR and adNR vulcanizates; a) NR, b) P10, c) P10-S12, d) P10-S25, e) P10-S37 and f) P10-S50.

3.2.4 Swelling in toluene

NR typically has poor resistance in non-polar solvent due to its hydrocarbon nature. Modification of NR by coating with PMMA-co-PMPS improved its swelling resistance in toluene. Table 7 shows the mole uptake of toluene, swelling index and soluble fraction for the NR vulcanizates, determined by immersion in toluene at room temperature for 5 days. All cases of adNR had significantly reduced uptake, swelling and soluble fraction relative to NR, with or without vulcanization. The cases with PMPS had the lowest values for these indicators that consistently decreased with PMPS content, indicating improved solvent resistance. This suggests that the number of

methoxy groups of PMPS was hydrolyzed and condensed to form siloxane bonds, which increased the network-chain density and increased in swelling resistance of adNR. The increment in network-chain density was calculated from crosslink densities, and is also shown in Table 7. The lowest swelling index value among the adNR vulcanizates were obtained with P10-S50, indicating the highest crosslink density

[28]. This is related to the molecular weight between crosslinks (M_c). The molecular weight between crosslinks for the admicelled samples was significantly lower than for NR, because the adNR contained PMPS that generated siloxane bonds during polymerization and increased the network-chain density. This observation is in line with the torque difference, which is also an indirect measure of crosslink density.

Table 7. Uptake of solvent, swelling index, soluble fraction, M_c and crosslink density across the samples, determined by immersion in toluene at room temperature for 5 days.

Cured Samples	Mole uptake (%)	Swelling index (%)	Solubility fraction (%)	M_c (g/mole)	Crosslink density $\times 10^{-5}$ (mole/cm ³)
NR*	1.05	96.90	46.68	3106889	0.0161
NR	0.84	77.60	3.69	21433	2.3329
P10	0.82	75.23	1.67	15920	3.1408
P10-S12	0.78	71.93	1.79	11591	4.3138
P10-S25	0.78	71.46	1.94	11130	4.4923
P10-S37	0.77	71.26	1.79	10888	4.5924
P10-S50	0.76	69.72	1.71	9451	5.2907

*No curing

3.2.5 Mechanical properties and aging

Mechanical properties of NR and adNR vulcanizates were summarized in Table 8. The tensile modulus slightly increased with PMPS loading. The incorporation of PMPS gives stiffer NR vulcanizates matching the increased crosslink density from siloxane. This result was attributed to the degree of crosslinking in shell as tensile modulus of the rubber vulcanizate is mainly dependent on the crosslink density. On the other hand, elongation at break significantly decreased with PMPS content due to the increase in chain stiffness from PMMA-co-PMPS in the NR leading to restrict the movement of polymeric chains upon stretching. There is no significant effect on the tensile strength and elongation at break between NR and adNR with PMMA 10 phr (P10). Although PMMA

is a rigid polymer, the incorporation of a small amount PMMA (8.63% of adNR with PMMA) into NR (89.32% of NR) does not affect the tensile strength and elongation at break of the P10. In cases of adNR with PMMA-co-PMPS, the tensile strengths of adNR vulcanizates tend to increase when PMPS is added. The result suggests that increasing rigid phases of PMPS with crosslinking in the rubbery matrix makes the composite more strength with lower ductility [29]. This behavior was attributed to the high degree of crosslink -Si-O-Si- in PMPS, as schematically showed in scheme 1 and confirmed by FTIR results.

In practical application, conventional fillers such as carbon black or silica are incorporated in NR for rubber reinforcement. In order to address potentiality of adNR, the

mechanical properties of adNR vulcanizates and NR filled precipitated silica were compared. Pattannawannidchai *et al.* [35], Norizahi *et al.* [36] and Sengloyluan *et al.* [37] reported mechanical properties of NR filled precipitated silica at 50 phr. Modulus, tensile strength and elongation at break of rubber vulcanizates were about 1.4-2.2 MPa, 9.9-20 MPa and 555-690%, respectively. It can be clearly observed that the modulus, tensile strength and elongation at break of adNR vulcanizates were comparable with those of NR filled with conventional silica.

The effect of coating on aging resistance, assessed from the mechanical properties of samples after accelerated aging at 70 °C for 96 h, is also reported in Table 8. The results reveal that aging at elevated temperature reduces tensile strength as well as elongation

at break. Regarding the tensile modulus, the results are not consistent. After aging the modulus of adNR vulcanizate was increased due to crosslink formation, whereas the modulus of NR decreased due to main chain scission by thermal oxidative reactions [30]. Both crosslink formation and main chain scission at high temperature reduce elongation at break. We have seen that the modulus slightly increased with aging due to additional crosslinks formed during accelerated aging. The additional crosslinks reduced elongation, but chain scission due to polymer degradation is evident from the loss of tensile strength [3]. However, adNR revealed less change in tensile strength, modulus and elongation at break suggesting that after encapsulated with PMPS, adNR vulcanizates provide better aging resistance as compared to NR.

Table 8. Mechanical properties and aging resistance of adNR vulcanizates.

Properties	Samples	Before	After aging	Retention (%)	Change (%)
Modulus (MPa)	NR	1.38 ± 0.15	0.83 ± 0.10	60.1	-39.9
	P10	1.43 ± 0.10	1.15 ± 0.08	80.4	-19.6
	P10-S12	1.46 ± 0.07	1.36 ± 0.07	93.2	-6.8
	P10-S25	1.53 ± 0.07	1.53 ± 0.07	100.0	0.0
	P10-S37	1.62 ± 0.02	1.62 ± 0.02	100.0	0.0
	P10-S50	1.64 ± 0.05	1.64 ± 0.05	100.0	0.0
Elongation at break (%)	NR	758 ± 20.2	274.3 ± 38.16	36.2	-63.8
	P10	727 ± 36.00	368.3 ± 35.97	50.7	-49.3
	P10-S12	536 ± 17.62	355.6 ± 97.69	66.3	-33.7
	P10-S25	523 ± 16.41	365.27 ± 38.12	69.8	-30.2
	P10-S37	478 ± 8.49	354.4 ± 23.13	74.1	-25.9
	P10-S50	452 ± 21.87	348.96 ± 51.10	77.2	-22.8
Tensile Strength (MPa)	NR	15.00 ± 0.04	2.01 ± 0.19	13.4	-86.6
	P10	14.14 ± 2.18	5.16 ± 0.88	36.5	-63.5
	P10-S12	16.49 ± 0.96	8.23 ± 0.69	49.9	-50.1
	P10-S25	18.17 ± 1.00	11.55 ± 0.39	63.6	-36.4
	P10-S37	19.08 ± 1.22	12.61 ± 0.48	66.1	-33.9
	P10-S50	19.55 ± 1.01	12.94 ± 0.30	66.2	-33.8

3.2.6 Dynamic mechanical properties

Dynamic thermal-mechanical analysis (DMA) can characterize the formation of siloxane linkages and the transition from glassy state to viscoelastic state. The storage modulus (E'), loss modulus (E'') and $\tan \delta$ are shown against temperature in Figure 9a-c, for the NR and adNR vulcanizates.

The storage modulus represents the elastic component in response, and indicates the capacity of a material to store deforming energy. As shown in Figure 9a, the modification of NR by coating with PMMA-co-PMPS increases the storage modulus of both in the glassy region and at ambient temperature. At low temperatures, the adNR is in glassy state and exhibits higher storage modulus than that of NR. The result implies that the degree of crosslink increases with adding PMPS due to the formation of siloxane linkages. As the temperature increased, the chains in NR vulcanizates became more mobile and lost their close packing arrangement, leading to decrease in the storage modulus at the glass transition (T_g) [31] at around -53°C to -45°C , as shown in Table 9. At temperatures above T_g , in the rubbery region from -53 to 100°C , the

storage modulus is higher for the adNR than for NR, because the added PMMA-co-PMPS restricts the mobility of rubber chains and hinders the movements of rubber segments, more so with higher PMPS contents. This also leads to progressive reduction in the maximum peak of loss tangent ($\tan \delta_{\max}$) [32], as seen in Figure 9c.

The maximum peak point of $\tan \delta$ is located at T_g , and these locations are summarized in Table 9. For unvulcanized NR, the T_g was found to be -53.0°C . The T_g of vulcanized NR shifted to -49.5°C . This is because crosslinking restricted the mobility of rubber chains and hindered the movements of rubber segments. The T_g values determined from $\tan \delta$ were further increased by coating of NR with PMMA-co-PMPS. This is due to the fact that the samples have more -Si-O-Si- linkages in shell, so their chain segments have rather hard mobilities. In addition, only one T_g was observed in each adNR sample suggesting that good miscibility of the three components was achieved in the core-shell structure produced by admicellar polymerization. This good miscibility was agree well with a single step degradation in TGA results.

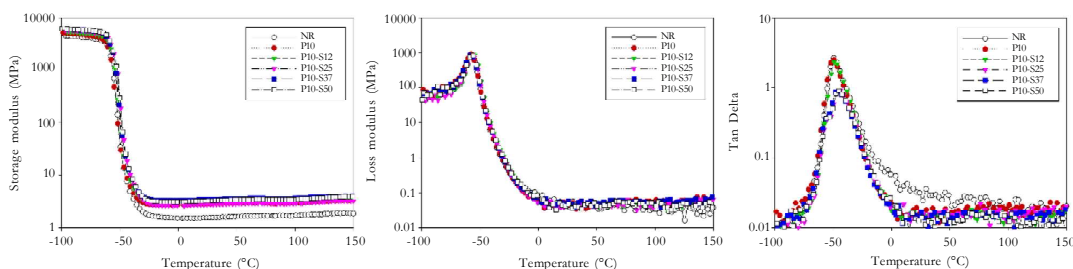


Figure 9. Dynamic-mechanical properties of NR and adNR vulcanizates.

Table 9. Storage modulus (E'), loss modulus (E'') and T_g estimate from DMA for the adNR vulcanizates.

Samples	E'		E''		$\tan \delta$		T_g (°C)
	-80 °C	-30 °C	-80 °C	-30 °C	-80 °C	-30 °C	
NR (No curing)	2455.84	0.62	33.16	0.083	0.013	0.134	-53.0
Cured NR	4177.11	1.55	64.69	0.055	0.016	0.036	-49.5
P10	4631.40	2.84	86.73	0.050	0.019	0.018	-49.3
P10-S12	5059.13	3.14	81.08	0.046	0.016	0.015	-49.1
P10-S25	5442.38	2.77	54.45	0.038	0.010	0.014	-46.6
P10-S37	5674.26	3.43	83.57	0.047	0.014	0.014	-45.2
P10-S50	5759.28	3.26	97.69	0.040	0.017	0.012	-45.0

4. CONCLUSIONS

NR modified with PMMA-co-PMPS was prepared by admicellar polymerization and then vulcanized by using sulfur in a conventional vulcanization system. During admicellar polymerization, hydrolysis and condensation of PMPS simultaneous with the free radical copolymerization of MPS and MMA gives rise to crosslinking the PMMA-co-PMPS shell, as confirmed by FT-IR and ^1H -NMR. The content of adNR in samples increased with PMPS content, according to Soxhlet extractions and XPS results. TEM confirmed the core-shell morphology of adNR while SEM revealed that rigid shell covering NR particles prevents NR fusion and crosslinking siloxane provides stability and maintained core-shell structure during processing. Good miscibility is also corroborated by only one T_g in the DMA properties and a single deformation in TGA results.

After vulcanization was applied to the adNR. The adNR vulcanizates had reduced solvent uptake, swelling index, and soluble fraction in toluene, and this solvent resistance and crosslinking improved with silane content. While some ozone cracks were found in all specimens, great improvement in ozone resistance was observed that consistently increased with PMPS content.

The improvement of ozone resistance also confirms that adNR was formed successfully. In addition, adNR vulcanizates showed higher tensile strength than that of NR and revealed less change in mechanical properties after aging suggesting better thermal resistance as compare to NR. Therefore, this adNR seems be an alternative material for developing a novel NR with adjustable properties for the various rubber industries.

ACKNOWLEDGEMENTS

This work was supported by Ratchadapiseksompoch Endowment and The Petroleum and Petrochemical College, Chulalongkorn University, Thailand. The authors were thankful to Prof. Brian P Grady (the School of Chemical, Biological and Materials Engineering, University of Oklahoma) for his help on NMR experimental and suggestion. The helpful suggestions by Assoc. Prof. Dr. Seppo Karrila from the Faculty of Science and Industrial Technology, Prince of Songkla University, Suratthani Campus, to improve a draft manuscript are gratefully acknowledged.

REFERENCES

- [1] Sombatsompop N. and Kumnuantip C., *J. Appl. Polym. Sci.*, 2006; **100**: 5039-5048. DOI 10.1002/app.23472.

- [2] Sitisaiyidah S., Lohyi E. and Nakason C., *Adv. Mater. Res.*, 2014; **844**: 437-440. DOI 10.4028/www.scientific.net/AMR.844.437.
- [3] Vinod V.S., Varghese S. and Kuriakose B., *Polym. Degrad. Stab.*, 2002; **75**: 405-412. DOI 10.1016/S0141-3910(01)00228-2.
- [4] Anancharungsuk W., Tanpantree S., Sruanganurak A. and Tangboriboonrat P., *J. Appl. Polym. Sci.*, 2007; **104(4)**: 2270-2276. DOI 10.1002/app.25661.
- [5] Saramolee P., Lopattananon N. and Sahakaro K., *Eur. Polym. J.*, 2014; **56**: 1-10. DOI 10.1016/j.eurpolymj.2014.04.008.
- [6] Wang Q., Luo Y., Feng C., Yi Z., Qiu Q., Kong L.X. and Peng Z., *J. Nanomater.*, 2012; **2012**: 1-9. DOI 10.1155/2012/782986.
- [7] Pongpilaipruet A. and Magaraphan R., *Mater. Chem. Phys.*, 2015; **160**: 194-204. DOI: 10.1016/j.matchemphys.2015.04.024.
- [8] Christopher K.R., Pal A., Mirchandani G. and Dhar T., *Prog. Org. Coat.*, 2014; **77**: 1063-1068. DOI 10.1016/j.porgcoat.2014.03.008.
- [9] Zou M., Wang S., Zhang Z. and Ge X., *Eur. Polym. J.*, 2005; **41**: 2602-2613. DOI 10.1016/j.eurpolymj.2005.05.038.
- [10] Huang K., Liu Y. and Wu D., *Prog. Org. Coat.*, 2014; **77**: 1774-1779. DOI 10.1016/j.porgcoat.2014.06.001.
- [11] Jang I.B., Sung J.H., Choi J. and Chin I., *J. Mater. Sci.*, 2005; **40**: 3021-3024. DOI 10.1007/s10853-005-2381-1.
- [12] Pongprayoon T., Yanumet N. and O'Rear E.A., *J. Colloid. Interf. Sci.*, 2002; **249(1)**: 227-34. DOI 10.1006/jcis.2002.8230.
- [13] Rungruang P., Grady B.P. and Supaphol P., *Colloid. Surface. A*, 2006; **275(1-3)**: 114-125. DOI 10.1016/j.colsurfa.2005.09.029.
- [14] Silakul P. and Magaraphan R., *Polym. Composite.*, 2017; 1-17. DOI 10.1002/pc.24648.
- [15] Magaraphan R. and Srinarang V., *J. Elastom. Plast.*, 2009; **41(5)**: 457-477. DOI 10.1177/0095244309340982.
- [16] Bunsomsit K., Magaraphan R., O'Rear E.A. and Grady B.P., *Colloid Polym. Sci.*, 2002; **280(6)**: 509-516. DOI 10.1007/s00396-001-0639-y.
- [17] Park B.D., Wi S.G., Lee K.H., Singh A.P., Yoon Y.H. and Kim Y.S., *Biomass Bioenerg.*, 2004; **27(4)**: 353-363. DOI 10.1016/j.biombioe.2004.03.006.
- [18] Lee M., Kim Y., Ryu H., Baeck S.H. and Shim S.E., *Polymer(Korea)*, 2017; **41(4)**: 599-609. DOI 10.7317/pk.2017.41.4.599.
- [19] Flory P.J. and Rehner J., *J. Chem. Phys.*, 1943; **11(11)**: 521-526. DOI 10.1063/1.1723792.
- [20] Poochai C., Pae-on P. and Pongpayoon T., *Int. J. Mater. Metallurg. Eng.*, 2010; **4(5)**: 346-350. DOI 10.13140/RG.2.1.1443.5280.
- [21] Zaioncz S., Dahmouche K., Paranhos C.M., San Gil R.A.S. and Soares B.G., *Express Polym. Lett.*, 2009; **3(6)**: 340-351. DOI 10.3144/expresspolymlett.2009.43.
- [22] Cai G.P. and Weber W.P., *Macromolecules*, 2000; **33(17)**: 6310-6314. DOI 10.1021/ma000390+.
- [23] Dai Q., Wu D.Z., Zhang Z. and Ye Q., *Polymer*, 2003; **44**: 73-77. DOI 10.1016/S0032-3861(02)00728-0.

- [24] Zhan X., Cai X. and Zhang J., *RSC Adv.*, 2018; **8**: 12517-12525. DOI 10.1039/c7ra13375h.
- [25] Rucigaj A., Krajnc M. and Sebenik U., *Polym. Sci.*, 2017; **3(2:9)**: 1-7. DOI 10.4172/2471-9935.100024.
- [26] Pereira Carvalho H.W., Suzana A.F., Santilli C.V. and Pulcinelli S.H., *Polym. Degrad. Stab.*, 2014; **104**: 112-119. DOI: 10.1016/j.polymdegradstab.2014.03.031.
- [27] Simma K., Rempel G.L. and Prasassarakich P., *Polym. Degrad. Stab.*, 2009; **94(11)**: 1914-1923. DOI 10.1016/j.polymdegradstab.2009.08.005.
- [28] Rohana Yahya Y.S., Azura A.R. and Ahmad Z., *J. Phys. Sci.*, 2011; **22**: 1-14. DOI 10.13140/RG.2.1.1419.5683.
- [29] Poompradub S., Thirakulrati M. and Prasassarakich P., *Mater. Chem. Phys.*, 2014; **144**: 122-131. DOI 10.1016/j.matchemphys.2013.12.030.
- [30] Sae-oui P., Sirisinha C. and Hatthapanit K., *Express Polym. Lett.*, 2007; **11(1)**: 8-14. DOI 10.3144/expresspolymlett.2007.3.
- [31] Pipattananukul N., Ariyawiriyanan W. and Kawahara S., *Energy Procedia*, 2014; **56**: 634-640. DOI 10.1016/j.egypro.2014.07.202.
- [32] Prasertsri S. and Rattanasom N., *Polym. Test.*, 2012; **31(5)**: 593-605. DOI 10.1016/j.polymertesting.2012.03.003.
- [33] Nelson P.A. and Kutty S.K.N., *Prog. Rubber Plast. Re.*, 2004; **20(3)**: 213-228. DOI 10.1081/PPT-200030065.
- [34] Yan H., Sun K., Zhang Yo., Zhang Yi and Fan Y., *J. Appl. Polym. Sci.*, 2004; **94**: 1511-1518. DOI 10.1002/app.21071.
- [35] Pattanawanidchai S., Loykulnant S., Sae-oui P., Maneevas N. and Sirisinha C., *Polym. Test.*, 2014; **34**: 58-63. DOI 10.1016/j.polymertesting.2014.01.002.
- [36] Norizah A.K. and Azemi S., *Asean J. Sci. Technol. Dev.*, 2017; **34(2)**: 57-56. DOI 10.29037/ajstd.399.
- [37] Sengloyluan K., Sahakaro K., Dierkes W.K. and Noordermeer J.W.M., *Express Polym. Lett.*, 2017; **11(12)**: 1003-1022. DOI 10.3144/expresspolymlett.2017.95.